Soft Matter

PAPER

View Article Online
View Journal | View Issue

Cite this: *Soft Matter*, 2025, **21**, 7803

Facile conversion of commercial silicones from thermoset to ultraviolet-set for increased processing versatility

Matthew R. Jamison,[a] Spencer Pak,[b] Eric J. Markvicka[bcd] and Stephen A. Morin*[aef]

Traditional platinum catalyzed hydrosilation chemistry used in thermoset silicones is ubiquitous in academic labs but has disadvantages in both curing time and the susceptibility of the catalyst to poisoning when exposed to common chemical species. This report presents the simple modification of commercial thermoset polydimethylsiloxane (PDMS) kits to yield ultraviolet (UV)-set silicones. The new UV-set characteristics take advantage of thiol–ene click chemistry to allow rapid and efficient curing while maintaining robust crosslinking chemistry supportive of comparable mechanical and chemical properties in the product material. The new UV-set formulation is easy to produce using commercially available reagents that are shelf stable and instantly convert thermoset kits (*e.g.*, Sylgard 184) to UV-set materials, broadly expanding the operational versatility of these silicones. The simple "UV part C" described here offers facile conversion of Sylgard 184 into a UV-set silicone that is compatible with traditional laboratory workflows (*e.g.*, soft lithography) and applicable to the production of liquid metal composites.

Received 7th July 2025,
Accepted 13th September 2025

DOI: 10.1039/d5sm00700c

rsc.li/soft-matter-journal

Introduction

Ubiquitous commercial silicone kits (*e.g.*, Sylgard 184 and EcoFlex), used extensively in the fields of soft robotics, stretchable electronics, and microfluidics, are limited to thermoset behavior.[1–4] This behavior restricts the application space accessible to these materials due to limitations including pot-life and cure speed. These commercial silicones, which have found wide-spread use in research labs, undergo thermoset behavior facilitated by a platinum catalyzed addition reaction between terminal vinyl groups and hydrosiloxane moieties present in the base (part A) and curing agents (part B) respectively.[5] While this reaction is well suited for many applications, as shown by its wide adoption in the research community, it is also limited by the nature of the platinum catalyst. This catalyst is known to be poisoned by the addition of thiols, amines, alkenes, and many other common chemicals.[6] This sensitivity limits the potential uses for these materials in advanced composites or when chemical modifications are desired. In this report we demonstrate a simple and accessible method for converting commercial platinum catalyzed silicones into ultraviolet (UV)-set systems. We demonstrated the utility of this system in executing and accelerating common laboratory workflows (*e.g.*, soft lithography) and in the production of advanced liquid metal composites.

Common methods to avoid the limitations caused by platinum catalyzed curing include pre-treatment of surfaces that contain these species or changing cure systems entirely, such as to tin catalyzed silicones.[7,8] These alternative systems offer some advantages over platinum-based systems, such as more resilient curing chemistry, but have tradeoffs including lower stability, release of molecules during curing, and health concerns.[9–11] In addition, these systems do not avoid the other limitations inherent to thermoset elastomers.

To combat the limitations of thermoset systems, several bespoke UV-set PDMS systems have been reported.[12–17] A common and well-known crosslinking method used by these bespoke systems is thiol–ene chemistry. The reaction between a thiol and an alkene to produce an alkyl sulfide is well

[a] *Department of Chemistry, University of Nebraska-Lincoln, Hamilton Hall, Lincoln, NE 68588, USA. E-mail: smorin2@unl.edu; Fax: +1(402) 472-9402; Tel: +1 (402) 472-4608*
[b] *Smart Materials and Robotics Laboratory, Department of Mechanical and Materials Engineering, University of Nebraska-Lincoln, Nebraska Hall, Lincoln, NE 68588, USA*
[c] *Department of Electrical and Computer Engineering, University of Nebraska-Lincoln, Nebraska Hall, Lincoln, NE 68588, USA*
[d] *School of Computing, University of Nebraska-Lincoln, Nebraska Hall, Lincoln, NE 68588, USA*
[e] *Nebraska Center for Materials and Nanoscience, University of Nebraska-Lincoln, Lincoln, NE 68588, USA*
[f] *Nebraska Center for Integrated Biomolecular Communications, University of Nebraska-Lincoln, Lincoln, NE 68588, USA*

understood and has been studied for decades.[18] This reaction is rapid, taking only seconds, especially when a photoinitiator is used, and has very high yield which can be near quantitative, often being classed as a type of "click" reaction.[19,20] A common approach to utilize this chemistry in polymer systems consists of the combination of vinyl terminated and thiol decorated chains which can be exposed to UV light to create a crosslinked network, including networks of silicone chains.[12,21] These materials avoid the problems associated with thermoset behavior and can be formulated to fill a variety of functions but can require multiple synthesis or formulation steps.[15,16] Some of this work has been driven by the additive manufacturing space which desires UV-set formulations for use in existing devices and workflows.[16,22] While some of these additive manufacturing resins are commercially available (*i.e.*, Silicone 40A resin from Formlabs) they are not extensively adopted by the research community, likely because they are formulated for specific applications rather than general lab use, the formulations are obscured to protect intellectual property rights, and they would require modifications to existing workflows designed for Sylgard 184 and similar systems. Sylgard 184 and other commercial silicones have been used as a base for a thiol–ene click resin, but these efforts focused on 3D printing capabilities, optimizing the resin properties using functionalized fillers and a crosslinking agent common to similar works but dissimilar to that used in commercial silicone kits.[23] Other prior work to generate UV-set silicones has typically been performed by mixing individual components and requires careful formulation for different applications. Neither approach lends itself to easy replacement of commercial silicones in existing laboratory workflows.

To avoid these limitations, we have produced a shelf stable "part C" addition to a common silicone system, Dow Chemical's Sylgard 184. This addition enables UV-set behavior but retains the commonly used thermoset behavior, allowing direct integration into existing workflows when more diverse functionality is desired. Our modification contains only commercially available off-the-shelf reagents and enables a drop-in modification of Sylgard 184 when UV-set properties or catalyst free conditions are preferred, enabling fast, efficient, and robust curing. We have designed our system to modify a commercial silicone kit to reduce the development and modifications needed for existing workflows. This formulation does not impart a significant increase in cost with a kilogram of UV-set PDMS costing less than 7% more than a kilogram of Sylgard 184. Notably this cost includes that of part B which is not used for the UV-set formulation. If the cost of part B is removed it will likely result in matching or reduced cost for a kilogram of UV-set PDMS when compared to thermoset PDMS.

We have formulated our part C to cure under affordable mobile light sources, such as a UV LED flashlight, to broaden the application space and ease of use for this modification. Additionally, we have demonstrated common soft lithography and microfluidic fabrication techniques to show the effectiveness of UV-set PDMS in common thermoset applications. Further, to illustrate the versatility and ease of our approach, we have developed liquid metal composites with opaque inclusions and demonstrated the advantages fast low-temperature curing can have on systems traditionally made with thermoset silicones.

Experimental

Materials

Dow Chemical Sylgard 184 elastomer kits (Ellsworth Adhesives), [4–6% (mercaptopropyl)methylsiloxane] – dimethylsiloxane copolymer (Gelest, CAS 102783-03-9), 1,3,5,7-tetravinyl-1,3,5,7-tetramethylcyclotetrasiloxane (Gelest, CAS 2554-06-5), xylene (Sigma Aldrich, CAS 1330-20-7), benzophenone (Sigma, CAS 119-61-9), hexanes (Sigma Aldrich, CAS 107-83-5), 2-propanol (Sigma Aldrich, CAS 67-63-0), SU8-2050 (Kayaku), SU8 Developer (Kayaku), and thermochromic powder (Comely11) were used without further modification. Gallium (RotoMetals) and indium (Indium Corp.) were combined at a 3 : 1 ratio by weight to produce EGaIn.

UV modification

We made our typical UV curing additive with mercaptopropyl co-dimethyl siloxane (MPPDMS) and a vinyl D4 silicone (vD4). If a photoinitiator was included, benzophenone was added as a 3 : 5 solution in xylene. We produced a UV-set silicone by mixing a commercial base (*e.g.* Sylgard 184 part A) in a 2 : 1 ratio with the UV-set component. UV samples were then set under 365 nm light for as little as 1 minute. UV sources used were a LightFe 365 nm UVM15 flashlight (30 W), a 1000 W Hg/Xe arc lamp (Newport, Irvine, CA, Model #6295NS), and a 90 W 95 × 95 mm Hg Grid Lamp (BHK, Ontario, CA, Model #88-9102-02). All samples were compared to Sylgard 184 prepared at a 10 : 1 (A : B) ratio and cured in a 60 °C oven for two hours.

Liquid metal composites

The liquid metal composite was fabricated by mixing EGaIn with the UV-set PDMS prepolymer in a planetary mixer (Flaktek, SpeedMixer DAC 400.2 VAC) at 1600 RPM for 1 minute. The emulsion was then poured into a mold and cured by exposing the composite to a 365 nm UV light source for 1 minute. Samples thicker than 1 mm sometimes required a longer curing time of 10 minutes. Microscope images of the cured composite samples were collected with a Zeiss Axio Zoom V16. Thermal conductivity was measured utilizing the transient plane source (TPS) method (Thermtest, MP-V) with 1 mm thick samples of various EGaIn volume loadings. To fabricate the thermal pattern revealing devices shown in Fig. 5, the liquid metal composite was first cast into the desired shape and placed in a Petri dish. The UV-set prepolymer was then poured around the sample to match its thickness. Finally, a thermochromic, UV-set PDMS prepolymer was cast over the sample to form a reporting layer. The reporting layer thickness was 5 mm. Each layer of the device was cured for 5 minutes. The device was placed on a hot plate at 60 °C and allowed to reach equilibrium. The sample was then placed on a stainless-steel cylinder cooled to −20 °C to act as a cold sink.

Mold fabrication

We modeled 3D printed molds with Inventor Professional and printed them with a Stratasys Dimension Elite 3D printer using ABS filament. We produced SU8-2050 masters by spin coating (3000 rpm for 60 seconds, ramp 300 s^{-1}) on an 80 mm diameter silicon wafer prebaked over 9 minutes with temperature ramping from 65 to 95 °C. We applied an edge-bead removal process during a second spin coating step (500 rpm for 30 seconds, ramp 100 s^{-1}, then 1000 rpm for 20 seconds) with SU8 developer. We then removed residual solvent by heating for 2 minutes at 65 °C. To pattern the mold a photomask (Fineline Imaging, Colorado Springs, CO) was applied along with a quartz plate to maintain contact between SU8 and the photomask during curing. Next, the prepared wafers were cured under the arc lamp until they achieved 110 mJ cm^{-2} of dosing. Finally, we performed a 7-minute post-bake step with temperature ramping from 65 to 95 °C. We removed uncured material by rinsing with SU8 developer for 6 minutes then isopropyl alcohol for 30 seconds.

Testing

We calculated the crosslink density and gel fraction by performing swelling experiments in a good solvent. To achieve this, we submerged the cured polymers in hexane for 72 hours, switching the solvent three times, and measured the initial mass of the polymer as well as the mass when swollen and after drying in a 110 °C oven for 24 hours. We then used these masses to calculate the crosslink density (γ_e) with the Flory–Rehner equation (eqn (1)), with a minimum of three samples for each value we reported.

$$\gamma_e = \frac{1}{2V_s}\frac{\ln(1-\phi_e)+\phi_e+\chi\phi_e^2}{\phi_e^{1/3}-\frac{\phi_e}{2}} \quad (1)$$

$$\chi = \frac{V_1}{RT}(\delta_1-\delta_2)^2 \quad (2)$$

$$\phi_e = \frac{m_{dry}/\rho_{PDMS}}{m_{dry}/\rho_{PDMS}+(m_{swollen}-m_{dry})/\rho_{solvent}} \quad (3)$$

Here the Flory–Huggins parameter (χ) is defined by eqn (2) and is calculated with the gas constant (R), the temperature (T), the molar volume of the polymer (V_1), and the Hildebrand solubility parameter of polymer (δ_1) and solvent (δ_2). We have taken the Flory–Huggins parameter to be zero between PDMS and hexane due to the similarity of the Hildebrand solubility parameters.[24] The variable ϕ_e is defined by eqn (3) and corresponds to the polymer volume fraction calculated with the mass of the dry (m_{dry}) and solvated ($m_{swollen}$) polymer along with the density of both solvent ($\rho_{sovlent}$) and polymer (ρ_{PDMS}). Variable V_s corresponds to the solvent molar volume (130 mL mol^{-1} for hexane). Gel fraction was calculated as the ratio of the dry polymer weight to the initial polymer weight.

We performed optical imaging on replica molded samples by pipetting a small amount of prepolymer on an SU8 master and flattening it with a Zehntner Testing Instruments applicator to achieve a final film thickness of 500 μm. Samples were then cured immediately with UV light and demolded with tweezers. Microscope images of these samples were taken with a Zeiss Axio Imager M2 equipped with a Calibri 7 light source and an Axiocam 712 Mono camera.

Mechanical properties were tested with an Instron 5944 universal testing instrument with a 100 N force transducer and pneumatic grips. To prepare samples for testing, we cast prepolymer into a Petri dish and cured. Cured samples were cut into strips which we individually measured with calipers before each test. We performed the mechanical tests at a strain rate of 254 mm min^{-1} (10 strain per min) for general mechanical properties while the shelf-life tests were performed at 80 mm min^{-1} (4 strain per min). We measured optical transmission with an Ocean Optics USB2000+ by placing a sample between two fiber optic leads with an attached Ocean Optics DH-mini source. Contact angle measurement were collected with a Biolin Scientific One Attention Theta goniometer using twelve measurements for each reported value.

Results and discussion

We have designed and tested a versatile crosslinking additive for Sylgard 184 which imparts UV-set functionality utilizing the existing chemical crosslinking handles with active thiol moieties. Rather than combining bespoke silicones and manually formulating vinyl terminated PDMS (vPDMS) and MPPDMS for individual synthesis, we have instead taken Sylgard 184 part A as the starting material and formulated a part C to enable UV-set behavior. This part C is primarily MPPDMS with 0.5% (v/v) vD4 and enabled UV-set behavior in ambient atmosphere under a low-pressure Hg grid lamp (184 nm, 256 nm) in minutes or a UV flashlight (365 nm) in a similar time (this formulation required the addition of 5% (v/v) photoinitator solution). The final samples were prepared by mixing Sylgard 184 part A with part C (2 : 1) and casting into a desired mold (Fig. 1). We chose to use MPPDMS as our crosslinking agent as it mirrors the chemical nature of the typical thermoset crosslinker present in Sylgard 184 part B (PHMS-*co*-PDMS) (poly(hydromethoxysilane-*co*-dimethylsiloxane)) which we expect to impart similar properties. We used a 2 : 1 ratio for this work to maximize both stress and strain at break, but other formulations were also tested and may be used for applications where different properties are desired (Table S1 and Fig. S1). This approach is similar to how different ratios of part A and B may be used to access different properties in traditional thermoset systems. This formulation was able to achieve significant gelation for a 3 mm thick sample in 15 seconds and full UV-set in as little as 30 seconds (360 mJ cm^{-2} at 365 nm using the Hg–Xe arc lamp).

We tested the mechanical properties of the new silicone material and found they were somewhat similar, especially under low strain (*i.e.* $\varepsilon < 1$) conditions common to many applications of Sylgard 184 (Fig. 2(A) and Fig. S2, S3). While similar, our unmodified formulation is softer (0.30 MPa vs 0.66 MPa), but with inclusion of a small amount of silica filler the gap can be reduced (0.52 MPa) and can also be reduced by using a stiffer formulation (0.46 MPa at a 3 : 2 ratio), detailed

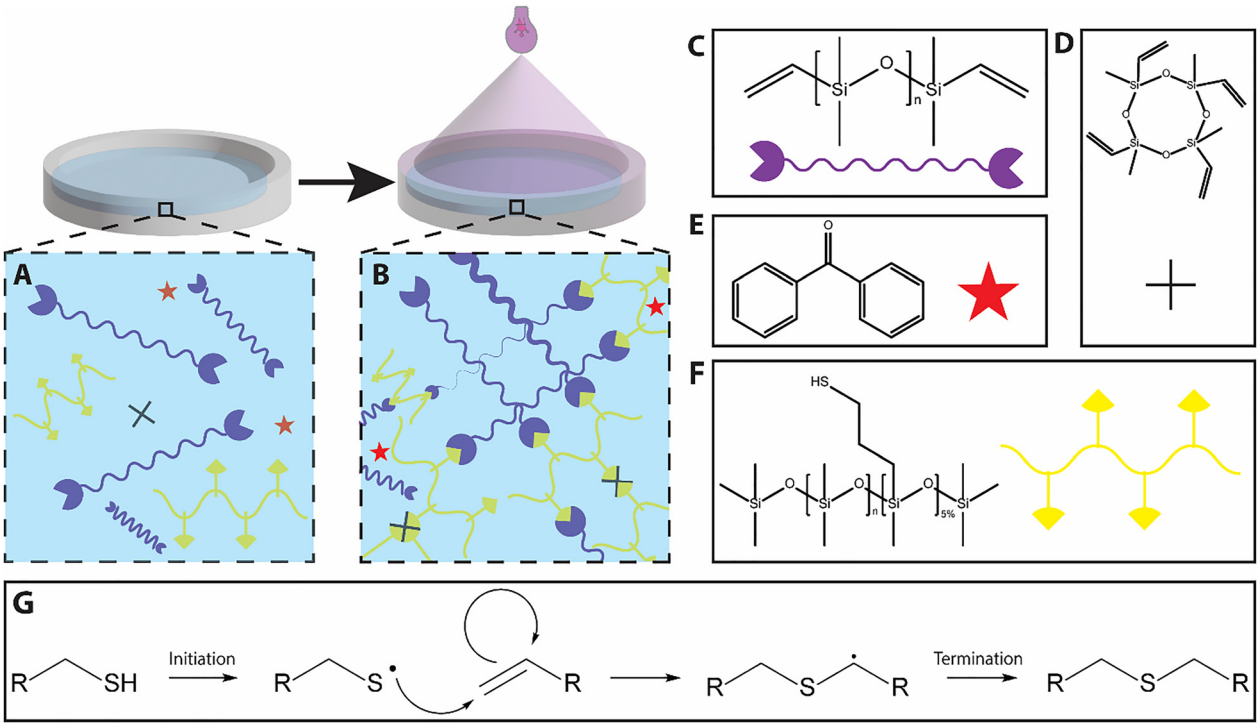

Fig. 1 Curing scheme of UV-set PDMS. (A) Prepolymer solution. (B) Cured UV-set PDMS. Chemical structures of the components of UV-set PDMS: (C) vPDMS, (D) vD4, (E) benzophenone, and (F) MPPDMS. (G) The thiol–ene reaction expected in our system.

mechanical data can be found in the supplementary information (Table S1). At higher strains the gap widens, likely from two main causes: lower filler content and decreased crosslink density. An important consequence of the method for formulation is a one third reduction in filler concentration present in the commercial kit, which would explain a gap in mechanical properties. To test this theory, we added 2.6 per hundred rubber untreated fumed silica to our final formulation and found the mechanical properties increased as expected, although not to the level of Sylgard 184. Part of the gap still present in the filled sample is due to the concentration of filler still being below that of Sylgard 184. We had difficulty further increasing the filler loading due to poor dispersion, and the remainder of the mechanical gap is likely due to the chemical nature of the filler used. Sylgard 184 is known to contain methyl vinyl functionalized silica (40–60% by mass) which will better disperse in the network, allowing more to be added, and actively participate in the chemical crosslinking, neither of which will happen with the untreated silica in our formulation.[6] Thus, if desired, more could likely be done to achieve closer mechanical properties using this method. For target applications in microfluidics, stretchable electronics, and soft robotics, the deviation from the mechanical properties of thermoset Sylgard 184 (namely the yield point and ultimate extensibility) are not a limitation since these applications require relatively low strains (in the range of 0.1–1).

The other likely cause of the disparity in mechanical properties is the final crosslink density. Given the nature of top-down UV curing one might expect a crosslink density gradient in the material from the side exposed to the UV to the side furthest from the UV source, which would affect the final mechanical properties; however, when tested we see no evidence of decreased crosslink density with increasing thickness up to 3.8 mm and instead see an increase in gel fraction indicating some cure inhibition at the surface, though tested samples were not tacky to the touch (Table S2). The decrease in gel fraction when compared to Sylgard 184 could limit some applications specifically in biological fields and may lower solvent stability. There is also a difference as the mobility of MPPDMS differs from the PMHS-*co*-PDMS typical of Sylgard 184 and the number of functional groups present in each chain is likely different. To confirm our hypothesis, we measured the crosslink density and found our formulation has about half as many crosslinks as Sylgard 184, although this discrepancy is likely smaller due to the aforementioned disparity in filler loading (Fig. 2(B)). We estimated the difference in crosslink density due to this effect by making the simple assumption that the weight of the filler can be removed from all parts of the Flory–Rehner equation. We performed this simple calculation for the high (60%) and low (40%) range of filler loading reported in the SDS of Sylgard 184. When adjusting for this approximation, a one third reduction in filler concentration, UV-set Sylgard is closer to that of Sylgard 184. This is especially true when it is considered the filler in Sylgard 184 is actively participating in network formation and therefore likely contributes more crosslink density than can be simply accounted for by the weight of the filler.

The viability of this formulation for general use as an additive to commercial silicones requires long-term stability.

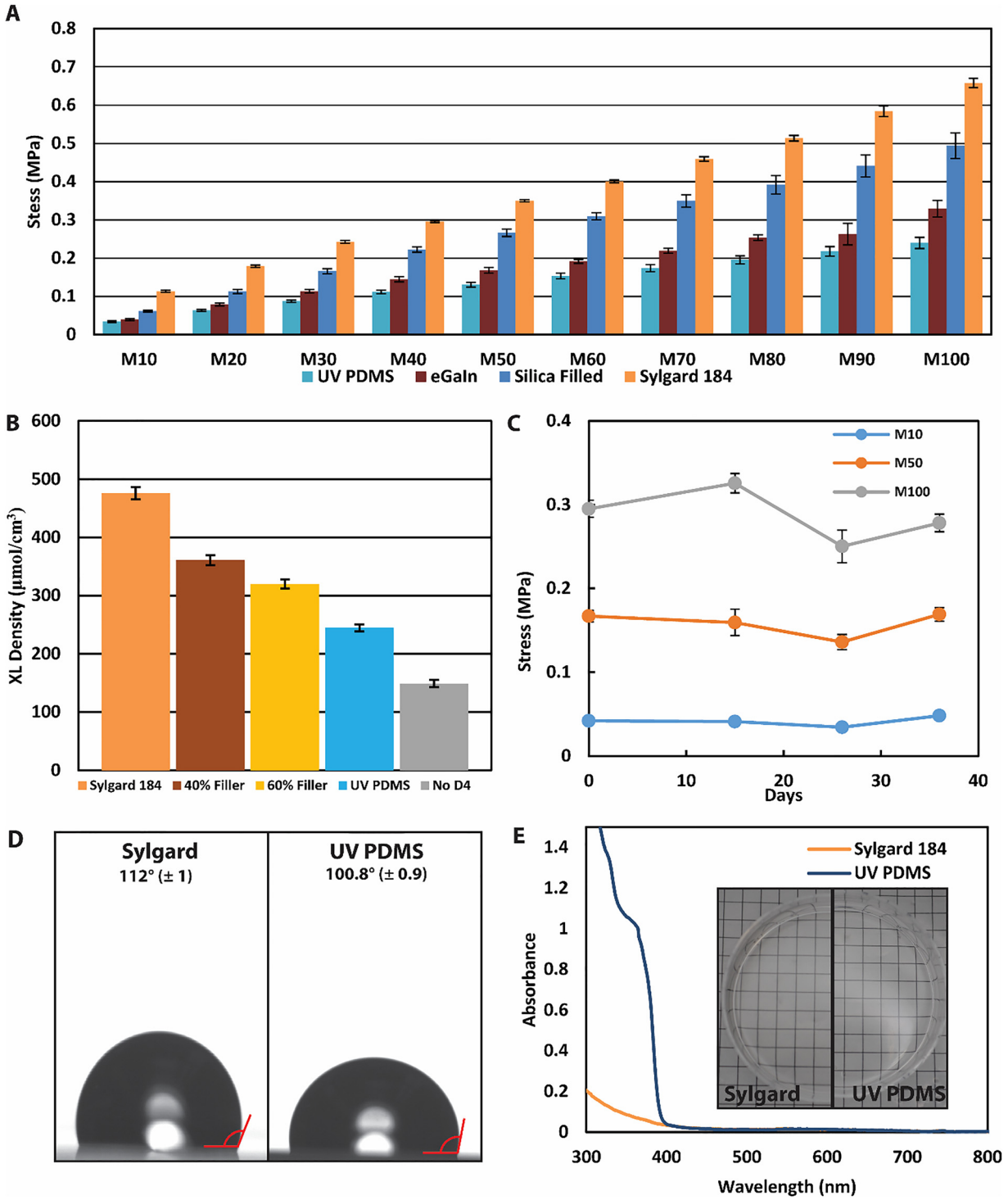

Fig. 2 (A) Tensile data of native and filled UV-set PDMS compared to Sylgard 184, MXX refers to the stress at a given strain (*e.g.* M100 is the stress at 100% strain). Error bars represent the standard deviation of the mean; the number of measurements is available in Table S1. (B) Crosslink density of UV-set PDMS with and without the addition of vD4 compared to Sylgard 184. The 40% and 60% samples represent Sylgard 184 with a simple correction for filler loading assuming 40% or 60% of the initial mass is silica filler. Error bars are propagated error for six samples. (C) Tensile data for UV-set PDMS made with UV part C over time. Error bars represent the standard deviation of the mean at the reported position for six samples. (D) Contact angle comparison between Sylgard 184 and UV-set PDMS. Error bars are standard deviations for 12 measurements. (E) UV-Vis data of Sylgard 184 and UV-set PDMS with an optical image insert (squares are 5 mm).

We made a batch of part C which we used to make and test UV-set PDMS over the course of a month to ensure stability in performance and found statistically insignificant changes at the 95% confidence interval in modulus over time as

determined by ANOVA tests (Fig. 2(C) and Fig. S4). Other important properties for applications of Sylgard 184 in research labs include surface chemistry and optical transparency. We measured the contact angle and found a small difference in surface energies (likely due to the free thiol groups present in the UV-set silicone) however, we tested common surface functionalization techniques (*e.g.*, O2 plasma bonding and silane functionalization) and found they still work well (Fig. 2(D)). The material also maintains optical transparency with the new formulation, only showing differences from Sylgard 184 below 400 nm due to the inclusion of benzophenone as a photoinitiator (Fig. 2(E)). Importantly, the surface of the sample does not feel tacky or different from that of thermally cured Sylgard 184 unless cured for a very short time (<1 min) where the surface can sometimes be slightly tacky.

To further demonstrate the applications of part C we have created a microfluidic device with common replica molding techniques (Fig. 3(A)). In brief, UV-set Sylgard 184 was poured into a master mold and set under 365 nm irradiation. If a sealed device was desired the molded PDMS was removed and activated along with a glass slide with oxygen plasma and the two were then placed in contact with each other for 15 minutes at 80 °C to seal the device. This technique is as versatile as typical replica molding workflows but takes a fraction of the time, notably only taking minutes while a traditional workflow would take hours, indicating promise for both rapid prototyping and mass production. We produced microfluidic devices with complex features such as interdigitated high aspect ratio structures to demonstrate the versatility of this technique (Fig. 3(B)). These devices were able to hold pressure and function in a robust manner consistent with that expected from thermoset Sylgard 184. We further demonstrated the versatility of this material by replication of microscale patterns as is often desired in soft lithography workflows (Fig. 3(C)). These patterns are well replicated, uniform, and are produced in less than a minute under irradiation from a 365 nm UV flashlight (Fig. 3(D)). We took cross-sectional images of these patterns to assess the quality of the replication process (Fig. 3(E) and (F)).

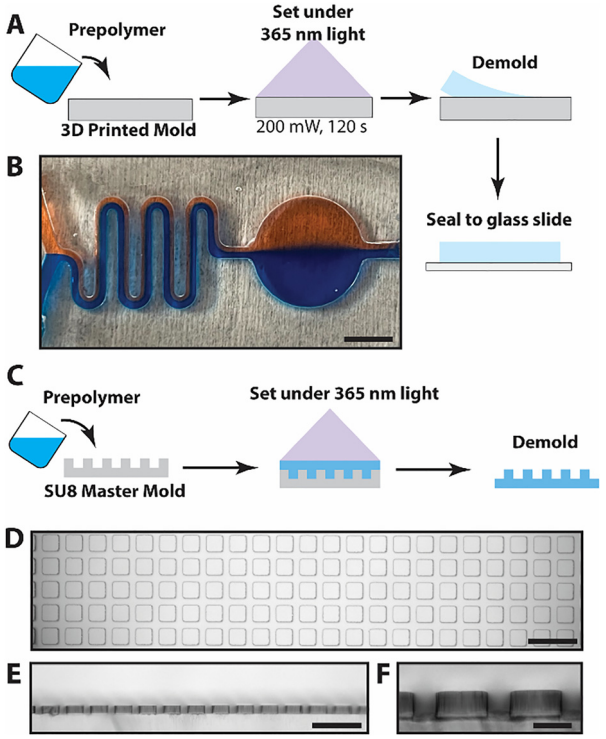

Fig. 3 (A) Schematic of bulk UV-set replica molding workflow. (B) Optical image of replica molded UV-set PDMS microfluidic device under 1 mL min^{-1} flow conditions. The scale bar is 5 mm. (C) Schematic of soft lithography UV-set workflow. (D) Microscope image of UV-set PDMS molded from an SU-8 Master with 50 μm squares. The scale bar is 200 μm. (E) Optical cross section of (D) with a 200 μm scale bar. (F) A closer cross section of (D). The scale bar is 50 μm.

In addition to the ability of UV-set PDMS to replicate existing workflows, two highly useful properties of UV-set PDMS are the rapid onset and robust nature of the cure. To further take advantage of these properties, we have produced a UV-set PDMS liquid metal composite (Fig. 4(A)). Traditionally thermal-set liquid metal composites can have issues with the dense liquid metal settling over the course of the cure.[25] While high temperatures can help to limit this effect, it is still present and requires an oven heated to a high temperature while our system is very fast and only requires an accessible UV flashlight. We have shown our UV-set PDMS can cure a few millimeters thick with up to 30 vol% liquid metal inclusions in minutes with no statistical disparity in size of particle between the top and bottom of the sample and a minor reduction in gel fraction (Fig. 4(B) and (C) and Table S2). Several loadings of liquid metal have been included and tested for thermal conductivity to demonstrate increased functionality (Fig. 4(D)). The robust curing chemistry could be further extended to include ligated metal particles, which commonly use thiol and amine ligands that can prevent traditional platinum curing, greatly increasing the application space for these materials.

We used the liquid metal composites to produce a pattern revealing device based on the thermal conductivity differences between liquid metal composites and unfilled UV-set PDMS (Fig. 5(A)). This device was able to be heated to slightly elevated temperatures to remove color and then placed on a cold sink to selectively color the patterned area (Fig. 5(B), (C) and SI Movies 1 and 2). The multi-layered device can be produced with robust chemical linking between all layers in fifteen minutes or less, further indicating the desirable properties of this material.

The versatility and qualities of UV-set PDMS further enables several new properties which can be useful for existing workflows. For example, the rapid nature of the cure allows potential application in additive manufacturing/printing. We demonstrated this possibility by writing an N on a glass plate under 365 nm light which we are then able to remove and manipulate (SI Movie 3). The rapid curing and nature of the thiol–ene click reaction also enables use of the prepolymer as a simple glue.[16] This glue is able to rapidly repair damage to existing devices and structures. We have demonstrated this effect by punching a 2.5 mm hole in the microfluidic device we produced previously.

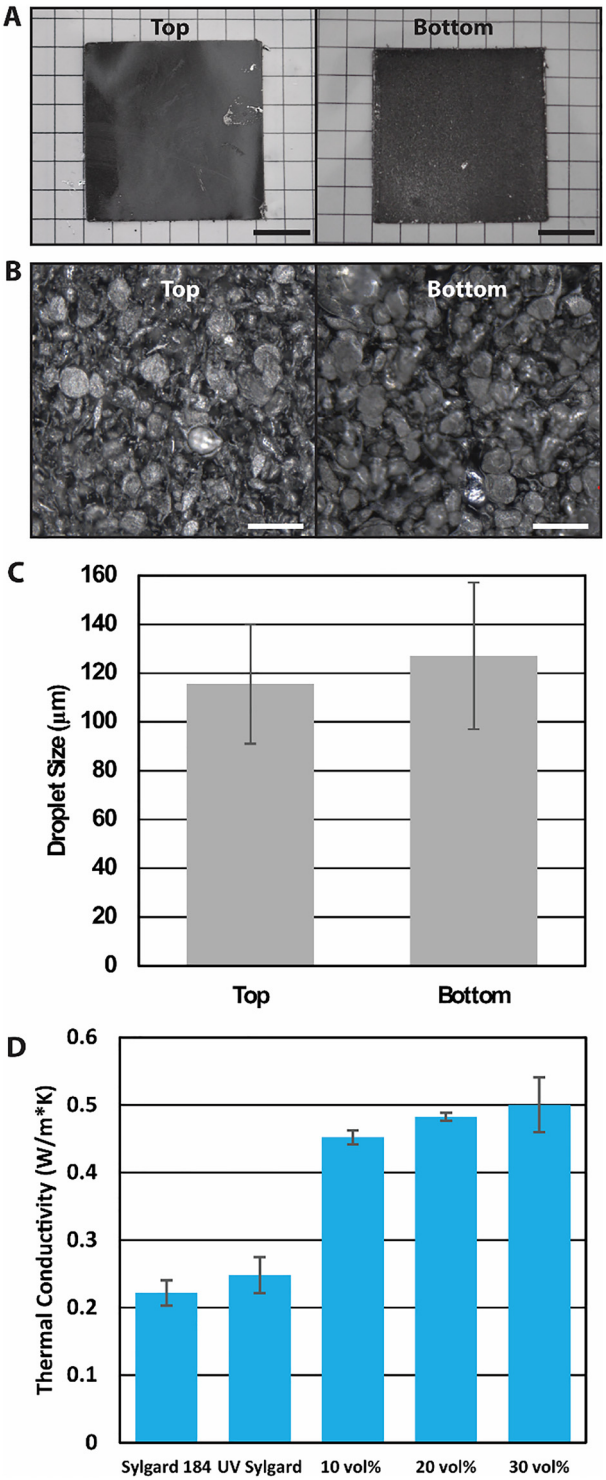

Fig. 4 (A) Optical image of the top and bottom the liquid metal composite, scale bars are 1 cm. (B) Microscope images of the top and bottom of a 20% filled sample, scale bars are 250 µm. (C) Particle size analysis of the droplets in (B) calculated with ImageJ. (D) Thermal conductivity as a function of sample composition. Error bars represent the standard deviation for 3 samples and 100 particles respectively.

This hole was able to be repaired to withstand previous flow conditions in under a minute by placing liquid prepolymer over the damaged area while under irradiation with a UV flashlight

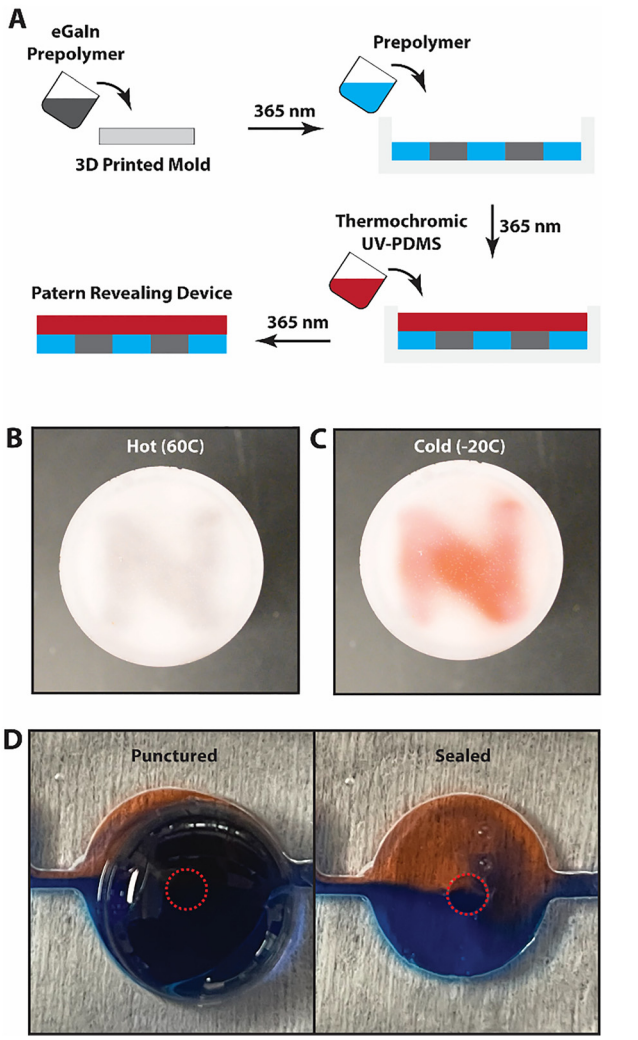

Fig. 5 (A) Schematic of thermal pattern revealing device fabrication. Optical images of the thermal pattern revealing device when warmed to 60 °C (B) and when placed on a −20 °C cold sink (C). (D) UV PDMS microfluidic device after puncturing with a 2.5 mm biopsy punch and subsequent rapid repair with UV PDMS. Red circles indicate the location of the punch.

(Fig. 5(D)). These techniques can also be extended to other silicone systems such as EcoFlex (Fig. S5).

Conclusions

We have developed an easily accessible UV part C for the widely used commercial silicone Sylgard 184 compatible with atmospheric UV-set conditions and widely accessible UV sources. Our part C requires minimal changes to existing workflows many labs have designed for Sylgard 184 and offers advantages in both time and energy efficiency while acting as a drop-in replacement for low strain applications. The demonstrated UV-set PDMS also circumvents common issues with addition cured silicones caused by catalytic poisoning and long cure times. To this end we have demonstrated the production of devices in minutes which would take hours to produce with traditional

thermoset systems (Sylgard 184) while maintaining typical device behavior. We have further demonstrated the use of our UV-set system to facilitate the fabrication of liquid metal composites with high liquid metal loadings for advanced devices while maintaining the ability to set in minutes despite the optical density. This simple modification has many advantages, with potential for additive, resource limited, and time limited manufacturing. In addition to the many fabrication advantages UV-set PDMS could provide, the material may also be used for rapid repair of existing devices and does not substantially increase the cost of PDMS use. Further, this formulation allows the selection of desired properties, labs can continue to use thermoset PDMS when desirable but can easily create UV-set material when it would be preferred. In principle, any lab working with Sylgard 184 could use this technique to improve efficiency and allow for production and investigation of new composite or chemically modified materials. This chemistry is also not limited to Sylgard 184 and will work for any platinum catalyzed thermoset PDMS kit.

Author contributions

M. R. J.: conceptualization; investigation; validation; writing – original draft; writing – review and editing. S. P.: investigation; writing – review and editing. E. J. M.: supervision; funding acquisition; writing – review and editing. S. A. M.: conceptualization; funding acquisition; supervision; writing – original draft; writing – review and editing.

Conflicts of interest

The authors declare no conflict of interest.

Data availability

The data that support the findings of this study are available from the corresponding author upon reasonable request.

Supplementary information containing tabulated mechanical data for all Sylgard 184 formulations and other commercial silicone formulations, stress–strain curves, and Movie 1–3 is available. See DOI: https://doi.org/10.1039/d5sm00700c.

Acknowledgements

M. R. J. and S. A. M. would like to acknowledge the Nebraska Center for Integrated Biomolecular Communication (P20GM113126) and the Nebraska Research Initiative for support. S. P. and E. J. M. would like to acknowledge support through the National Science Foundation (No. CMMI-2339780), National Aeronautics and Space Administration (80NSSC24M0139), and the Nebraska Tobacco Settlement Biomedical Research Development Fund.

References

1 F. Ilievski, A. D. Mazzeo, R. F. Shepherd, X. Chen and G. M. Whitesides, *Angew. Chem., Int. Ed.*, 2011, **50**, 1890–1895.
2 D. Qi, K. Zhang, G. Tian, B. Jiang and Y. Huang, *Adv. Mater.*, 2021, **33**, 2003155.
3 K. Raj M and S. Chakraborty, *J. Appl. Polym. Sci.*, 2020, **137**, 48958.
4 S. Pak, M. D. Bartlett and E. J. Markvicka, *Adv. Funct. Mater.*, 2024, **34**, 2410908.
5 R. Y. Lukin, A. M. Kuchkaev, A. V. Sukhov, G. E. Bekmukhamedov and D. G. Yakhvarov, *Polymers*, 2020, **12**, 2174.
6 D. Ortiz-Acosta, *Sylgard® Cure Inhibition Characterization*, Los Alamos National Laboratory (LANL), Los Alamos, NM United States, 2012.
7 B. Venzac, S. Deng, Z. Mahmoud, A. Lenferink, A. Costa, F. Bray, C. Otto, C. Rolando and S. Le Gac, *Anal. Chem.*, 2021, **93**, 7180–7187.
8 C. McConville, G. P. Andrews, T. P. Laverty, A. D. Woolfson and R. K. Malcolm, *J. Appl. Polym. Sci.*, 2010, **116**, 2320–2327.
9 A. Jurásková, K. Dam-Johansen, S. M. Olsen and A. L. Skov, *J. Polym. Res.*, 2020, **27**, 1–14.
10 F. W. van Der Weij, *Macromol. Chem. Phys.*, 1980, **181**, 2541–2548.
11 F. Gubbels, *Int. J. Adhes. Adhes.*, 2024, **132**, 103728.
12 K. Goswami, A. L. Skov and A. E. Daugaard, *Chem. – Eur. J.*, 2014, **20**, 9230–9233.
13 M. A. Cole and C. N. Bowman, *J. Polym. Sci., Part A: Polym. Chem.*, 2012, **50**, 4325–4333.
14 X. Jiao, J. Liu, J. Jin, F. Cheng, Y. Fan, L. Zhang, G. Lai, X. Hua and X. Yang, *ACS Omega*, 2021, **6**, 2890–2898.
15 S. Menasce, R. Libanori, F. B. Coulter and A. R. Studart, *Adv. Mater.*, 2024, **36**, 2306494.
16 T. J. Wallin, J. H. Pikul, S. Bodkhe, B. N. Peele, B. C. M. Murray, D. Therriault, B. W. McEnerney, R. P. Dillon, E. P. Giannelis and R. F. Shepherd, *J. Mater. Chem. B*, 2017, **5**, 6249–6255.
17 N. Bhattacharjee, C. Parra-Cabrera, Y. T. Kim, A. P. Kuo and A. Folch, *Adv. Mater.*, 2018, **30**, 1800001.
18 T. Posner, *Ber. Dtsch. Chem. Ges.*, 1905, **38**, 646–657.
19 H. C. Kolb, M. G. Finn and K. B. Sharpless, *Angew. Chem., Int. Ed.*, 2001, **40**, 2004–2021.
20 C. E. Hoyle and C. N. Bowman, *Angew. Chem., Int. Ed.*, 2010, **49**, 1540–1573.
21 C. F. Carlborg, T. Haraldsson, D. Öberg, M. Malkoch and W. van der Wijngaart, *Lab Chip*, 2011, **11**, 3136–3147.
22 N. Zheng, Z. Fang, W. Zou, Q. Zhao and T. Xie, *Angew. Chem., Int. Ed.*, 2016, **55**, 11421–11425.
23 M. Schaffner, J. A. Faber, L. Pianegonda, P. A. Rühs, F. Coulter and A. R. Studart, *Nat. Commun.*, 2018, **9**, 878.
24 J. N. Lee, C. Park and G. M. Whitesides, *Anal. Chem.*, 2003, **75**, 6544–6554.
25 T. V. Neumann, E. G. Facchine, B. Leonardo, S. Khan and M. D. Dickey, *Soft Matter*, 2020, **16**, 6608–6618.

